Journal of Fluorescence (2019) 29:1171–1181
https://doi.org/10.1007/s10895-019-02433-w

ORIGINAL ARTICLE

Multiplatform Protein Detection and Quantification Using Glutaraldehyde-Induced Fluorescence for 3D Systems

Mariana I. Neves[1,2,3] · Marco Araújo[1,2] · Cristina C. Barrias[1,2,4] · Pedro L. Granja[1,2,3,4] · Aureliana Sousa[1,2]

Received: 23 July 2019 / Accepted: 27 August 2019 / Published online: 6 September 2019

Abstract

Glutaraldehyde (GTA) is a dialdehyde used as biological fixative and its interaction with proteins like bovine serum albumin (BSA) has been well described. Additionally, GTA is known to induce fluorescence when interacting with BSA molecules. In this work, it is developed a new sensitive and reproducible method for BSA quantification using GTA crosslinking to endow fluorescence to BSA molecules. This method can be used with standard lab equipment, providing a low cost, fast-tracking and straightforward approach for BSA quantification. Techniques such as confocal laser scanning microscopy (CLSM) and spectrofluorometry are applied for quantitative assessment, and widefield fluorescence microscopy for qualitative assessment. Qualitative and quantitative correlations between BSA content and GTA-induced fluorescence are verified. BSA concentrations as low as 62.5 μg/mL are detected using CLSM. This method can be highly advantageous for protein quantification in three-dimensional hydrogel systems, specially to evaluate protein loading/release in protein delivery or molecular imprinting systems.

Keywords Bovine serum albumin · Biosensor · Hydrogels · Confocal laser scanning microscopy · Spectrofluorometry

Introduction

Glutaraldehyde ($C_5H_8O_2$, GTA) is an organic compound widely used as fixative agent and crosslinker. This dialdehyde was initially used as a biological fixative for cytochemistry and electron microscopy in 1963 by Sabatini et al. [1] and later in the preparation of protein crystals for X-ray diffraction studies and enzyme immobilization [2]. Nowadays, GTA is used for multiple purposes in biosensor [3, 4] and bio-absorbent [5–8] applications and for the improvement of absorption or selectivity of materials such as cellulose [3], chitosan [5, 6], alginate [7], polyanaline [4] or polyethyleneimine [8]. Crosslinking with GTA is also frequently used to enhance mechanical properties of different materials, including starch [9], collagen [10], gelatin [11–14], chitosan [13], amongst others [15, 16] for tissue engineering, wound healing or drug delivery applications.

Since the early 1960's, several studies focused on understanding and describing the interaction between GTA and proteins [17–21]. Protein-aldehyde bonds formed via GTA are usually higher in number and more stable than with other aldehydes, exhibiting high resistance to temperature and acid treatments [18]. Besides, GTA crosslinking of proteins can occur under physiological conditions of pH [19, 21], ionic strength [22] and temperature [23], representing an important advantage in biological and biomedical applications. This reactivity towards proteins is, in fact, reported to be favored by GTA 5-carbon structure and molecular size [18, 21]. GTA-protein interactions generally occur through ε-amino groups of amino acids, particularly lysine residues [17] with each lysine residue binding 3 GTA molecules [18, 21]. This can be the reason why fixation using GTA is able to better retain

Pedro L. Granja and Aureliana Sousa contributed equally to this work.

Electronic supplementary material The online version of this article (https://doi.org/10.1007/s10895-019-02433-w) contains supplementary material, which is available to authorized users.

✉ Aureliana Sousa
filipa@ineb.up.pt

[1] i3S - Instituto de Investigação e Inovação em Saúde, Universidade do Porto, Rua Alfredo Allen 208, 4200-135 Porto, Portugal

[2] INEB - Instituto de Engenharia Biomédica, Universidade do Porto, Rua Alfredo Allen 208, 4200-135 Porto, Portugal

[3] FEUP- Faculdade de Engenharia da Universidade do Porto, Universidade do Porto, Rua Dr Roberto Frias s/n, 4200-465 Porto, Portugal

[4] ICBAS - Instituto de Ciências Biomédicas Abel Salazar, Universidade do Porto, Rua de Jorge Viterbo Ferreira 228, 4050-313 Porto, Portugal

enzymatic activity when compared to other fixating agents [1] as lysine residues are usually not present in the catalytic center [2]. Other functional groups also known to have reactivity towards GTA are α-amino, guanidinyl, secondary amino and hydroxyl groups [2].

Being available at high purity rates and low costs, bovine serum albumin (BSA, ~66 kDa) is widely used as a model protein [24, 25] in the most varied fields of research. BSA contains 59 lysine residues [26] many of them able to interact with GTA through their ε-amino groups. Interactions between GTA and BSA, amongst other proteins, have been reported in several studies that focused on understanding GTA effects on protein activity and underlining mechanisms of GTA fixation [17, 19].

In 2016, Ma et al. explored the GTA ability to crosslink BSA to develop a protein hydrogel exhibiting green ($\lambda_{ex}/\lambda_{em}$ = 470/530 nm) and red ($\lambda_{ex}/\lambda_{em}$ = 595/630 nm) fluorescence for biomedical applications [27]. The hydrogel could be tested both in vitro and in vivo without the need of additional fluorescent labels [27]. The authors suggested that the observed hydrogel fluorescence resulted from electronic π-π* transitions of C=C bond and n-π* transitions of C=N bond from GTA oligomers and resultant Schiff base product, respectively [27].

This work proposes a novel protein quantification method based on GTA crosslinking induced-fluorescence, using BSA as model protein. The method was developed to overcome limitations of some commercially available methods, namely sample processing and high costs. Significantly, in contrast to most commercial kits, the method herein described can be used not only to quantify free protein molecules in solution, but also proteins immobilized in/on a substrate that does not need to be sacrificed. To demonstrate this, alginate modified with methacrylate groups was used as model hydrogel for BSA immobilization by entrapment. This material showed to be an appropriate model to test the proposed quantification method by enabling protein quantification without the need for sample processing. On the other hand, these alginate hydrogels could be solubilized, returning the protein to its free form, which was key for allowing direct comparison of the new method with established ones. Besides providing quantitative analysis of data by confocal laser scanning microscopy (CLSM) and spectrofluorometry, this method also allows fast-tracking qualitative analysis of samples using simpler widefield fluorescence imaging systems.

Experimental Section

Preparation of Hydrogel Precursor Solutions

Precursor solutions were obtained by sequentially dissolving sodium chloride (NaCl) and 2-hydroxy-1-[4-(hydroxyethoxy)phenyl]-2-methyl-1-propanone (photoinitiator Irgacure 2959, Sigma-Aldrich) in DI water to obtain a 0.9% (*w*/*v*) NaCl, 0.05% (w/v) Irgacure 2959 solution (photoinitiator solution). Then, bovine serum albumin (BSA, ~66 kDa, Sigma-Aldrich) was dissolved and sequentially diluted in the photoinitiator solution in order to obtain varying BSA concentrations [0–1% (*w*/*v*)]. Finally, alginate methacrylate (ALMA, **Experimental S1**) was dissolved in these solutions at a final concentration of 2% (w/v).

Production of GTA-Crosslinked ALMA Hydrogel Discs with Varying Amounts of BSA

Hydrogel discs were produced using a Teflon-spacer-glass based system. Briefly, 20 μL of precursor solutions were pipetted to a Teflon substrate with 500 μm spacers and a glass was placed on top. Photopolymerization was induced by exposing samples to 7 mW/cm2 UV light (320–395 nm, BlueWave 200 Light-Curing Spot Lamp, Dymax, adjusted using ACCU-CAL-30 Smart UV intensity Meter, Dymax) for 180 s. After production and depending on the experiment, hydrogels were incubated in 6.25, 12.50 or 25 wt% GTA (ON, 4 °C). Protein concentrations used in formulations were specifically 0, 6.25×10^{-3}, 12.50×10^{-3}, 25×10^{-3}, 50×10^{-3}, 0.125, 0.25, 0.5 or 1% (*w*/*v*) BSA.

Swelling Ratio

Hydrogel discs were weighted before and after incubation in 25 wt% GTA (ON, 4 °C). Swelling ratio (SR) was calculated using the following eq. (1):

$$SR = (w_{GTA} - w_0)/w_0 \quad (1)$$

were w_{GTA} (mg) is the disc weight after GTA incubation and w_0 (mg) is the initial disc weight, i.e., upon production (t = 0).

Scanning Electron Microscopy (SEM)

Hydrogels with 0 and 1% (*w*/*v*) BSA and incubated ON (4 °C) in 25 wt% GTA or phosphate buffered saline (PBS, pH 7.4) were rinsed twice in deionized water, snap frozen in liquid N2 and lyophilized. Prior to image acquisition, samples were coated with Au/Pd and images acquired under under high vaccum (Quanta 400 FEG ESEM / EDAX Genesis X4M).

Fourier-Transform Infrared (FTIR) Spectroscopy

Hydrogels after incubation in 25 wt% GTA were dried under vacuum for 24 h and then analysed as KBr pellets (1 wt% dried hydrogel to KBr). Each sample was analyzed from 4000 to 400 cm^{-1} with 4 cm^{-1} resolution (Perkin-Elmer 2000).

Preparation of Samples for Confocal Laser Scanning Microscopy (CLSM)

Hydrogel discs were incubated in 6.25, 12.50 or 25 wt% GTA. Prior to observation, samples were removed from GTA incubation solution and rinsed twice in PBS (pH 7.4) solution to remove any unreacted compounds. Excess of PBS in discs was removed. Discs were immersed on Vectashield mounting medium (VECTOR Laboratories) prior to observation.

CLSM Image Acquisition

Images were acquired on a laser confocal microscope (TCS-SP5 AOBS, Leica Microsystems) using LCS software (Leica Microsystems) applying fixed parameters (magnification, laser intensity, smart gain, offset and pinhole) that were maintained throughout all experiments performed on the same protein concentration range and the same GTA incubation solution. For instance, experiments using 6.25 wt% or 12.50 wt% GTA would have settings differently adjusted to avoid image saturation or signal loss, but such settings would remain the same throughout independent experiments for the same preparation conditions. Images were acquired in three different channels: channel 0 (C0, blue) using $\lambda_{ex} = 405$ nm and $\lambda_{em} = 418–500$ nm, channel 1 (C1, green) using $\lambda_{ex} = 488$ nm and $\lambda_{em} = 502–583$ nm, and channel 2 (C2, red) using $\lambda_{ex} = 561/594$ nm and $\lambda_{em} = 614–687$ nm. For each sample, 10 different stacks were obtained at approximately the middle height of the disc and recorded for approximately 60 μm z-height.

CLSM Image Quantification

A Z-projection of all stacks (max intensity) was performed using ImageJ software (ImageJ, version 1.50b; Rasband, W.S.). In each projected image, 6 measurements of Mean Gray Value (A.U.) of disc region and 6 measurements of the background region were obtained for each channel (Fig. S1).

Protein Quantification with Commercial Kits. Hydrogel discs were weighted and dissolved in 250 μL of a 0.1 M NaOH solution for approximately 45 mins (RT). Protein quantification was performed using DC Protein Assay (Bio-Rad) and Pierce BCA Protein Assay (ThermoFischer Scientific). For each assay performed in a 96-well plate, a calibration curve was obtained by dissolving protein in the NaOH solution and performing successive dilutions [0–0.1% (*w*/*v*) BSA]. All samples were prepared according to the manufacturer guide and absorbance values were read at $\lambda = 750$ nm and $\lambda = 562$ nm for DC and BCA kits, respectively.

Widefield Fluorescence Imaging

Image acquisition was performed using ZOE Fluorescent Cell Imager (Bio-rad) in brightfield and fluorescence channels (blue channel: $\lambda_{ex} = 355/40$ nm and $\lambda_{em} = 433/36$ nm; green channel: $\lambda_{ex} = 480/17$ nm and $\lambda_{em} = 517/23$ nm; red channel: $\lambda_{em} = 556/20$ nm and $\lambda_{em} = 615/61$ nm). Samples prepared as for CLSM experiments. Acquisition settings maintained for all acquisitions.

Spectrofluorometry

Hydrogel precursor solutions were produced with final concentrations of 0.2% (*w*/*v*) ALMA, 0–0.1% (w/v) BSA and 2.5 wt% GTA in ultrapure water (18 MΩ, Milli-Q UltraPure Water System, Millipore). Excitation ($\lambda_{em} = 510$, 550 and 590 nm) and emission spectra ($\lambda_{ex} = 465$ nm) were obtained using quartz cuvettes (1 nm increment, Horiba Fluoromax-4 Spectrofluorometer). For direct fluorescence reading and protein quantification in polymeric material, discs were produced and incubated alike for CLSM, rinsed twice in PBS (pH 7.4) and plated in 96-well black plates (Greiner Bio-one). Area scan readings obtained with $\lambda_{ex}/\lambda_{em} = 465/510$ nm (1 nm increment, BioTek's Synergy™ Mx Microplate Reader) and the average of 13 values/well used to perform the quantifications.

Statistical Analysis

Data was analyzed using GraphPad Prism 6 software for Windows, (GraphPad Software, San Diego California USA) by unpaired t-test with Welch's correction (99% confidence interval). For comparison with theoretical values, significance was tested using a one-sample t-test (99% confidence interval). Statistically significant differences are marked with * ($p < 0.05$), ** ($p < 0.01$), *** ($p < 0.001$) and **** ($p < 0.0001$).

Results and Discussion

GTA Crosslinking Effect in BSA/ALMA Hydrogel Discs

To analyze the effect of GTA crosslinking and BSA presence on the hydrogels, discs were characterized concerning their initial weight and swelling ratio after incubation in 25 wt% GTA solution (Fig. 1a). Discs containing varying amounts of protein presented similar initial weights: 18.00 ± 0.71, 16.23 ± 1.30, 16.80 ± 0.96, 17.02 ± 0.95 and 16.83 ± 0.68 mg for 0, 0.125, 0.25, 0.5 and 1% BSA, respectively (Fig. 1a-i). After overnight incubation in GTA, the hydrogel discs showed a trend for lower swelling ratios in formulations with higher amounts of BSA, with statistically significant differences in 0.5 and 1% BSA-containing discs, when comparing to discs

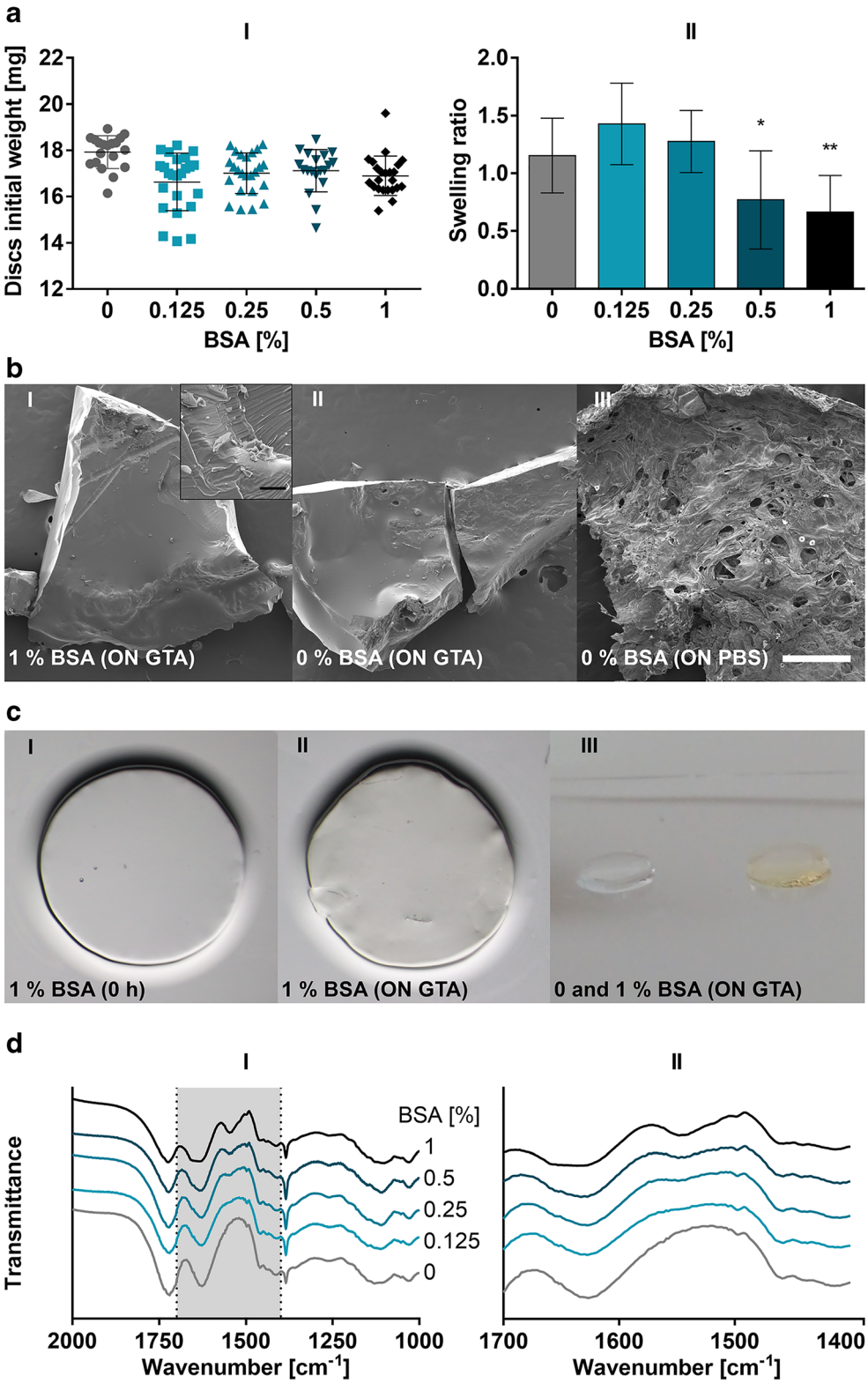

Fig. 1 Morphological and structural characterization of discs with 0–1% BSA, before and after incubation in 25 wt% GTA (ON, 4 °C). **a** Discs weight upon production (A-I) and swelling ratio of discs after incubation in GTA (A-II). Ticks and bars represent mean values ± standard deviation ($n = 3$). Asterisks represent statistical differences comparing to 0% BSA condition. **b** SEM images of samples incubated in GTA (B-I and B-II) and PBS (B-III) [scale bar 500 μm (white) and 10 μm (black)]. **c** Images of discs with 1% BSA before (C-I) and after (C-II) incubation in GTA and comparison of discs with 0% BSA (left) and 1% BSA (right) after incubation in GTA. **d** Representative FTIR spectra of discs with 0–1% BSA after incubation in GTA (D-I) with detailed view of the gray region (400–1700 cm-1, D-II)

without BSA (0%) (Fig. 1a-II). Such observation may be explained by the interaction between entrapped BSA and GTA molecules [2]. At higher levels of protein molecules, more reactive sites are available to interact with GTA, possibly leading to crosslinking degrees that start affecting the swelling behavior of the ALMA polymer mesh. Nevertheless, at lower protein values (0.125 and 0.25%), such interactions were not enough to significantly decrease the polymer swelling behavior. In fact, in both 0.125 and 0.25% BSA-containing discs, swelling ratios were slightly higher than discs without protein.

Even though such differences were not significant, this may be an indicator that BSA promoted osmotic flow. Since at these protein levels the crosslinking effects of GTA were not strong enough to counteract with the swelling events, the diffusion inwards the disc led to a slight increase in swelling ratio when comparing to discs with no protein.

Differences in porosity could not be confirmed by SEM (Fig. 1b). Samples incubated in 25 wt% GTA containing both 0% BSA (Fig. 1b-i) or 1% BSA (Fig. 1b-ii) presented a glass-like, brittle structure with no macro or microscopic pores. This apparent structure is not the typical structure observed in hydrogels [28] where networks with intricate porosity are usually present, as observed in samples solely incubated in PBS (Fig. 1b-III). This may be the result of GTA interaction with the carbohydrate molecules constituting the hydrogel. As previously referred, GTA crosslinking has been used to improve carbohydrate materials, including alginate [29, 30]. Alginate-GTA interaction has been studied and characterized before [31, 32] and is thought to occur between cis-oriented vicinal hydroxyl groups of alginate monomers and GTA, resulting in covalent crosslinking via acetal links [31, 33]. Even though these microscopic features may be a result of alginate-GTA interaction, as they appear in samples with and without protein, macroscopic features, particularly color, seem to result solely from GTA-BSA interaction (Fig. 1c). After production, all hydrogel discs were initially transparent, but discs containing protein became yellowish after incubation in GTA (Fig. 1c-I and II). Differences in color became more pronounced as the protein content increased, being particularly noticeable in 1% BSA samples and absent in 0% BSA samples (Fig. 1c-III). This is in accordance with existing literature [17, 27] where others described the presence of a straw color in solutions were GTA reacted with BSA, ovalbumin and human gamma globulin [17].

For further physicochemical characterization, FTIR analysis was performed. The obtained spectra (Fig. 1D-I and II), showed the formation of a new peak around 1545 cm^{-1}, accompanied by the formation of a shoulder around 1650 cm^{-1}, with increasing concentrations of BSA. These peaks are characteristic of the combination between the C-N stretching and N-H bending vibrations in amides (amide II) and C=O stretching vibrations in amides (amide I), respectively [34, 35]. Comparing the intensity of both peaks, it seems that the formation of the Schiff base characteristic from the GTA-BSA reaction may also be responsible by the increased intensity of the peak at 1545 cm^{-1}, since C=N stretching vibrations in imines usually appear between 1530 and 1550 cm^{-1} [36, 37]. Possible interactions between GTA and hydroxyl moieties of alginate cannot be discarded, resulting in the formation of an acetal ring with a characteristic peak around 1250 cm^{-1} [32, 36]. Here, the intensity of this peak decreased with the increasing amount of BSA available for reaction, which is comprehensible regarding the higher nucleophilic strength of amines when compared to hydroxyl groups. Overall, FTIR results confirmed the successful entrapment of BSA within ALMA hydrogel discs and suggest a possible interaction between BSA and GTA during incubation [32, 36, 38].

BSA Quantification by GTA-Induced Fluorescence Using CLSM

In order to evaluate if BSA-fluorescence induced by GTA crosslinking [27] could be qualitatively/quantitatively correlated with the amount of protein present in discs, hydrogels containing 0–1% BSA were incubated in GTA and observed by CLSM using three channels (C0, C1 and C2) at different λ_{em} and λ_{ex}. Acquired images were then analyzed using ImageJ software and results are shown in Fig. 2. Qualitatively, it was possible to detect a decrease in fluorescence concomitant with the decrease in protein content in all channels (Fig. 2a). While in samples with higher amounts of BSA (0.5 and 1%) the fluorescence in the discs was clear, as protein content decreased (0.125 and 0.25%) it became progressively more difficult to distinguish the discs from the background. In GTA-crosslinked discs without protein, the disc and background regions were nearly indistinguishable. In these cases, after image acquisition, post-processing setting adjustment (contrast and brightness) were only performed to define the limits of the disc, as it can be observed in the insets of Fig. 2a.

A quantitative analysis was then performed by measuring fluorescence in terms of Mean Gray Value (Mean, A.U.) (Fig. 2b-I and -II). Linear regressions were determined fitting the Mean values obtained for each channel and protein content (Fig. 2b-I), which returned equations with coefficient of determination (R^2) of 0.8915, 0.9963 and 0.9603 for C0, C1 and C2, respectively. A direct proportional increase of fluorescence (i.e., Mean values) with protein content was therefore confirmed, particularly for C1 ($\lambda_{ex}/\lambda_{em}$ = 488/502–583 nm). C1 was also the channel presenting higher sensitivity for protein detection, as confirmed by the greatest equation slope (3.18 units) when comparing to C0 and C2 (2.50 and 2.10 units, respectively). As expected, samples with higher protein content presented higher fluorescence (Fig. 2b-II) in all channels, with statistically significant differences between samples of different protein content (Table S1). These results agree with the FTIR and CLSM qualitative observations, confirming that differences in fluorescence were related with differences in protein content. It is noteworthy that CLSM data was obtained from measures of four independent experiments, supporting the fidelity of the method, namely for C1. Sample preparation and observations were performed separately and in different days, to take into account inherent experimental variability. Additionally, even though the same acquisition settings were used, fluctuations in laser power may occur throughout the same day or between different days. The

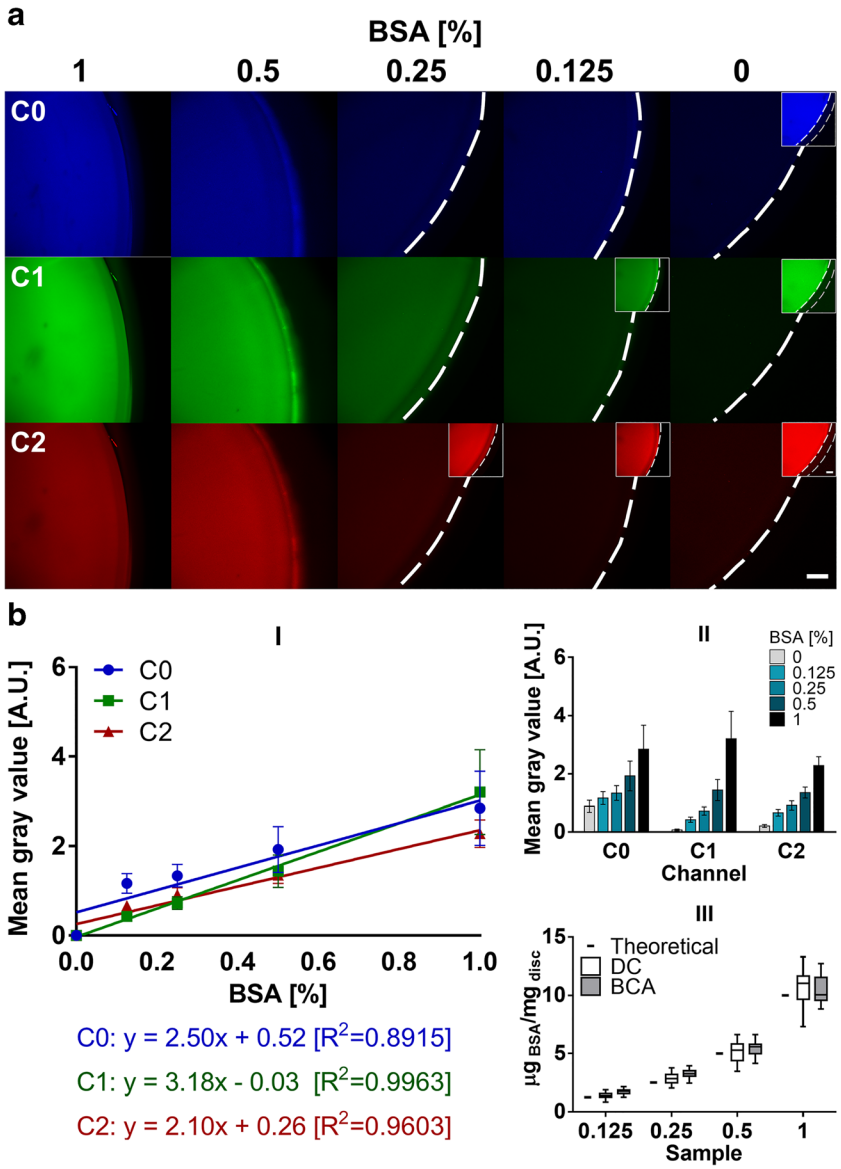

Fig. 2 CLSM data of GTA-induced BSA-fluorescence of discs with 0–1% BSA and incubated in 25 wt% GTA (ON, 4 °C). Data for channels C0, C1 and C2. **a** representative CLSM imaged discs. Insets represent the same image treated with ImageJ automatic (Auto) increase of Bright/Contrast to discriminate the disc and its border. Scale bar represents 200 μm. **b**-I linear regressions and corresponding equation and R^2 obtained from Mean Gray Values measures of CLSM images obtained and (**b**-II) comparison between Mean Gray Values of discs with 0–1% BSA. **b**-III comparison between theoretical values of protein content and data obtained from DC and BCA protein quantification kits (sample name correlates with protein content). Bars and symbols represent mean values ± standard deviation ($n = 4$), with exception for theoretical value (absolute)

use of different sample dishes could also create variance in the final results, but that did not occur. Despite all variances derived from independent experiments, R^2 values for C1 remained satisfactory for a reliable correlation between protein content and fluorescence, attesting the robustness and replicability of the proposed method.

Protein content of the hydrogels was confirmed using two commercially available protein quantification kits, DC and BCA (Fig. 2b-III), after sample processing to solubilize ALMA covalently crosslinked chains. The amount of protein present in discs (μg BSA/ mg disc) was determined and then compared to the expected theoretical values (Fig. 2b-III and Table S2). For 0–0.5% BSA samples, DC retrieved the lower and the closest to the theoretical values, while BCA retrieved lower standard deviations in all conditions. Values retrieved for 0.125 and 0.25% BSA samples by both methods were statistically different from the theoretical values and were also statistically different between each other. However, no statistical difference was found between values retrieved for both methods for 0.5 and 1% BSA samples (**Table S2**). Since analyzed samples were prepared simultaneously for both protein quantification methods, differences regarding the theoretical values can result from sample processing steps, such as hydrogel dissolution or sample dilution. On the other hand, differences between the two protein assay kits may be due to the inherent characteristics of each assay.

To evaluate if the amount of GTA could be decreased, while still allowing BSA-quantification by CLSM, lower concentrations of GTA were tested (6.25 and 12.50 wt%) (Fig. 3). In both cases it was still possible to qualitatively perceive differences in fluorescence between samples with different protein amounts (Fig. 3a). However, such differences were

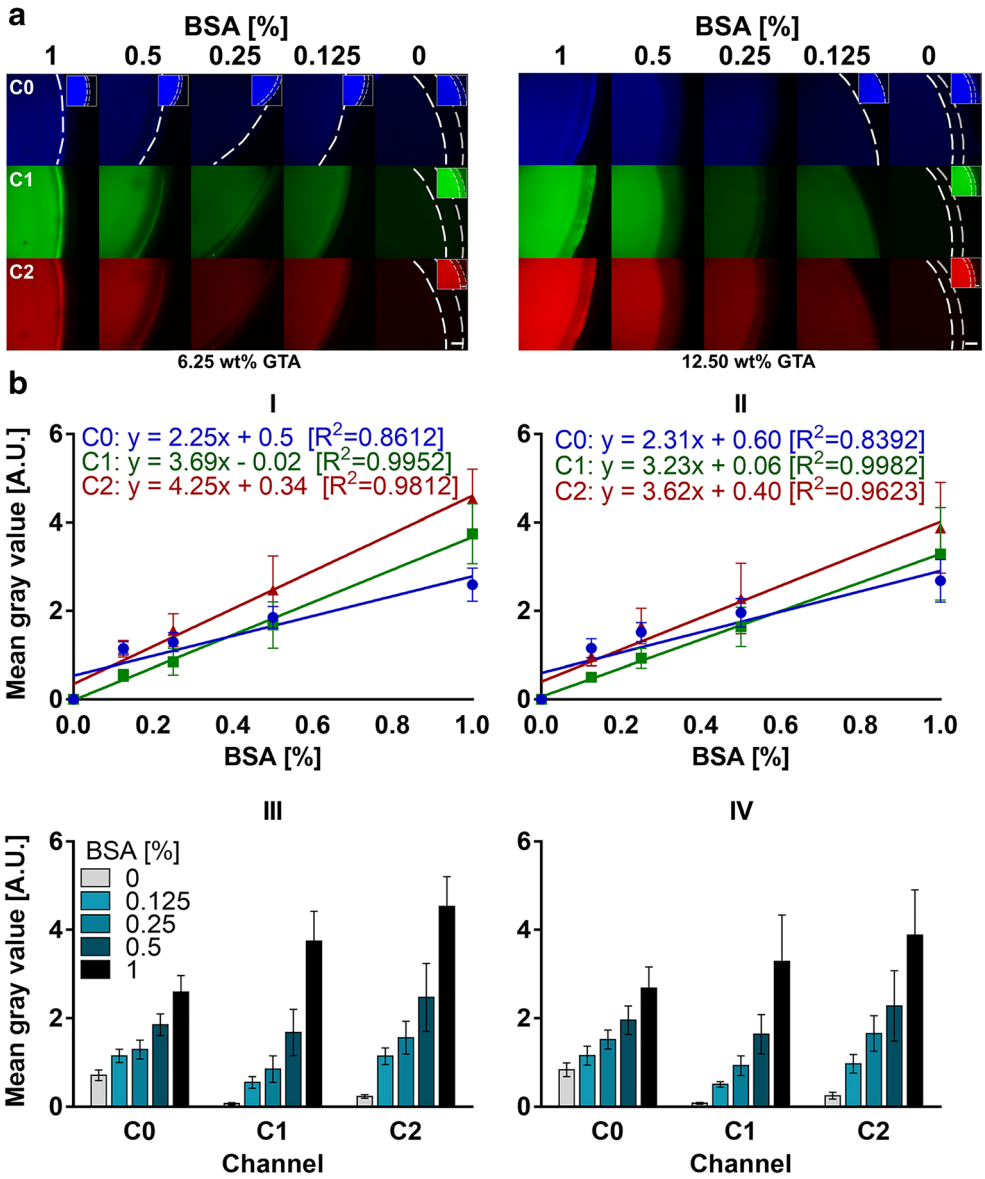

Fig. 3 CLSM data of GTA-induced BSA-fluorescence of discs with 0–1% BSA and incubated in 6.25 and 12.50 wt% GTA (ON, 4 °C). Data for channels C0, C1 and C2.
a representative CLSM imaged discs. Insets represent the same image treated with ImageJ automatic (Auto) increase of Bright/Contrast to discriminate the disc and its border. Scale bar represents 200 μm. **b** linear regressions and corresponding equation and R^2 obtained from Mean Gray Value measures of CLSM images obtained for 6.25 (**b**-I) and 12.50 (**b**-II) wt% GTA and comparison between Mean Gray Values of discs with 0–1% BSA for 6.25 (**b**-III) and 12.50 (**b**-IV) wt% GTA. Bars and symbols represent mean values ± standard deviation ($n = 3$)

not so evident as those obtained with 25 wt% GTA. Linear regressions fitting the Mean values measured (Fig. 3b-I and II) showed once again C1 retrieving the highest R^2 value (0.9952 for 6.25 wt% GTA and 0.9982 for 12.50 wt% GTA), as opposed to R^2 values for C0 and C2 (0.8612 and 0.9812 for 6.25% and 0.8392 and 0.9623 for 12.50 wt%, respectively). R^2 values followed the same trend despite the GTA concentration used, with $R^2_{C1} > R^2_{C2} > R^2_{C0}$. However, with lower GTA concentration, the C2 equations presented slightly higher slope than C1, while there was still independence between Mean readings of samples with different protein content (Fig. 3b-III and IV), as confirmed by the statistical analysis presented in Table S3.

In order to confirm if protein concentration could be further decreased and still be detectable by CLSM, we produced hydrogels with 10x lower BSA concentrations (0–0.125%). These were incubated in 25 wt% GTA and subsequently observed under CLSM with settings adjusted accordingly (Fig. 4). Once again, the same trend of fluorescence was observed as in previous experiments regarding qualitative (Fig. 4a) and quantitative (Fig. 4b) assessment of the obtained images. C1 retrieved again the higher R^2 value (0.9947) when compared to C0 (0.9847) and C2 (0.9554), changing therefore the R^2 tendency to $R^2_{C1} > R^2_{C0} > R^2_{C2}$ as opposed to the previous experiments using higher protein contents where this tendency was $R^2_{C1} > R^2_{C2} > R^2_{C0}$. Thus, decreasing protein content seems to influence more the accuracy of C2 channel than changing GTA concentration. This may be a result of BSA being the limiting factor of the reaction instead of GTA, which is most likely present in excess. Of significance is the high disparity between linear regression slopes, further confirming the higher sensitivity of C1 channel towards

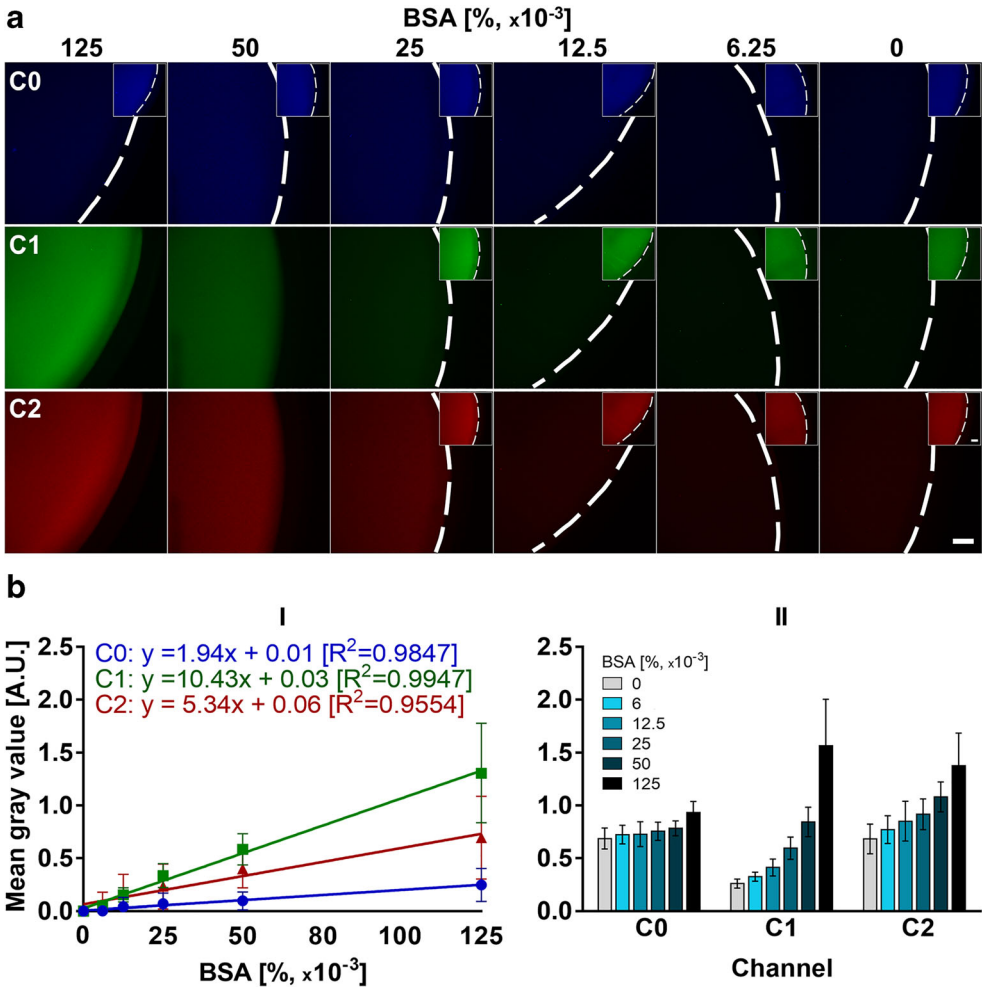

Fig. 4 Minimum levels of BSA fluorescence detected by CLSM. Analysis of samples with 0–0.125% BSA and incubated in 25 wt% GTA. Data for channels C0, C1 and C2. **a** representative CLSM imaged discs. Insets represent the same image treated with ImageJ automatic increase of Bright/Contrast to show the presence of the disc and its border. Scale bar represents 200 μm. **b**-I linear regressions and corresponding equation and R^2 obtained from Mean Gray Value measures of CLSM images obtained and **b**-II comparison between Mean Gray Values of discs with 0–1% BSA. Bars and symbols represent mean values ± standard deviation ($n = 3$)

changes in protein content in comparison with the other two channels. Whereas in the previous experiments (Figs. 2b-I and 3b-I and II) the differences in slopes obtained for each channel were never more than 1 unit apart, at this protein concentration range C1 presented a slope value 5.38 times larger than C0 slope and 1.95 times larger than C2 slope (Fig. 4b-I). This data supports the idea that C1 λ_{ex} and λ_{em} range is the most sensitive towards GTA-induced BSA fluorescence. Loss or reduction of sensitivity with protein content for C0 and C2 was also confirmed by statistical analysis of the data (Table S4). In the particular case of C0, no significant differences in fluorescence were detected in samples with consecutive protein concentrations. In C2, this discrimination was also lost between 12.50 vs. 25×10^{-3}% BSA and was reduced bellow 12.50×10^{-3}% BSA when comparing to C1. Thus, protein concentrations as low as 6.25×10^{-3}%, and eventually lower (not tested), can still be detected with this method if C1 conditions ($\lambda_{ex}/\lambda_{em}$ range) are used. This is not very far from the working range of DC (Bio-Rad, 5–250 μg/mL [39]) and BCA (Thermo Scientific, 20–2000 μg/mL [40]) commercial kits. Additionally, CLSM enables to analyze protein spatial distribution inside bulk materials, since several stacks of the sample can be observed. This may be quite convenient for the analysis of proteins inside 3D hydrogel systems, especially if they are transparent and thus optimal for CLSM imaging. In particular, the method provides a useful tool to evaluate protein loading or release in systems developed for applications such as protein delivery [41, 42] or molecular imprinting [43].

BSA Quantification by GTA-Induced Fluorescence Using Widefield Microscopy and Spectrofluorometry

Other methods were tested to analyze differences in GTA-induced BSA-fluorescence, such as qualitative analysis using a ZOE Fluorescent Cell Imager (Bio-rad) (Fig. 5a). This method allowed a very fast (down to 30 min incubation time), low cost and easy procedure to distinguish between samples with or without BSA. However, it did not allow visual discrimination of fluorescence between samples with different BSA content.

Spectrofluorometry was tested as an alternative quantitative method. A preliminary study was developed based on the

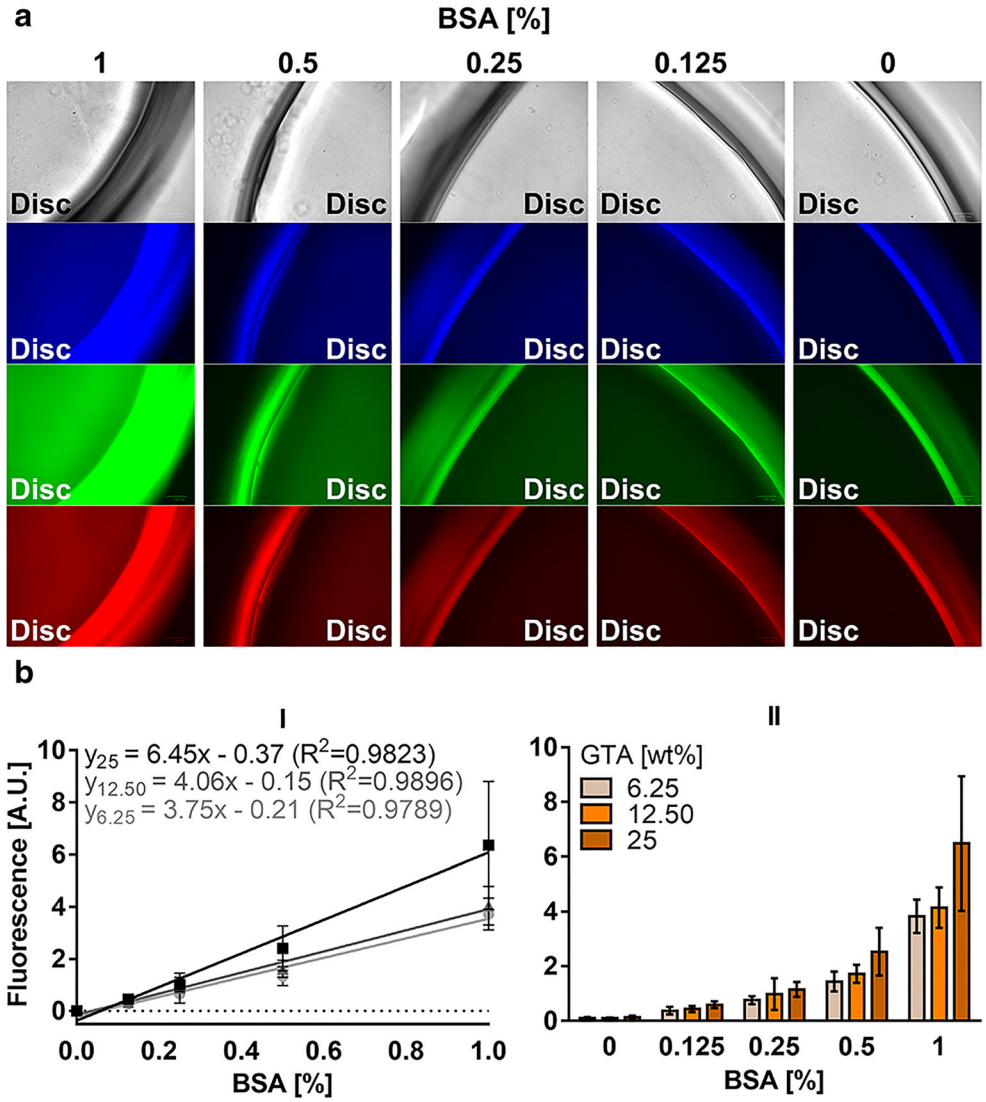

Fig. 5 Widefield fluorescence imaging and spectrofluorometry data GTA-induced BSA-fluorescence. (A) representative images acquired in widefield microscope Zoe Fluorescent Cell Imager of samples with 0-1 % BSA, (ON, 4 °C) in 25 wt% GTA. (B) spectrofluorometry data (λex/λem 465/510 nm) directly measured in discs: (B-I) linear regressions and corresponding equations and R2; (B-II) fluorescence comparison of discs with 0-1 % BSA incubated in 6.25, 12.50 or 25 wt% GTA (ON, 4 °C). Bars and symbols represent mean values ± standard deviation (n=3)

work of Ma et al. [27] who detected the existence of specific emission peaks, namely λ_{em} = 510, 550 and 602 nm, under optimal excitation wavelengths. Herein, tests were performed using solutions containing all the components of the system (hydrogel precursor solution) diluted 10x, i.e., 0.2% ALMA and 0–0.1% free BSA, with 2.5 wt% GTA. Firstly, excitation spectra of solutions containing 0.1% BSA were obtained using λ_{em} = 510 nm, 550 nm and 590 nm to determine their optimal excitation wavelengths. These wavelengths were within the λ_{em} range that retrieved better results in CLSM studies, where channel C1 ($\lambda_{ex}/\lambda_{em}$ = 488/502–583 nm) returned the most accuracy and sensitivity. It was possible to observe (Fig. S2a) that for all λ_{em} tested, two main excitation regions appeared, approximately between 330 and 390 nm and 455–477 nm. However, it was mainly between 455 and 477 nm that a well-defined peak region appeared, which was more pronounced for λ_{em} = 510 nm, with a maximum excitation peak detected around λ_{ex} = 465 nm. This agrees with the CLSM results, where C1 channel (λ_{ex}/ λ_{em} = 488/502–583 nm) retrieved better correlation between protein content and fluorescence levels (Fig. 2). Such excitation peak was also dependent on the presence of protein in the tested solutions, with higher protein concentrations retrieving higher fluorescence intensity (Fig. S2b). On the other hand, by the analysis of the emission spectra λ_{ex} = 465 nm (Fig. S2c), an emission peak region (λ_{em} = 508–518 nm) occurred that was more pronounced with

increasing protein concentrations, also in agreement with the CLSM results obtained for C1. Fluorescence readings in the peak region were fit in a linear regression correlating with protein levels as low as 125 μg/mL of free BSA, obtaining a R^2 value of 0.9948. Thus, $\lambda_{ex}/\lambda_{em}$ = 465/510 nm were the chosen conditions to proceed with fluorescence measures directly in discs. Hydrogels containing 0–1% BSA were further incubated in 6.25, 12.50 or 25 wt% GTA and fluorescence was measured. Linear regressions and absolute fluorescence readings are presented in Fig. 5b. The accuracy of this method is slightly lower than the one obtained with CLSM for the parameters used, with R^2 values reaching 0.9789, 0.9896 and 0.9823 for 6.25, 12.50 or 25 wt% GTA, respectively. Sensitivity increase was concomitant with the increase in GTA concentration, with experiments using 25 wt% GTA returning an equation slope of 6.45 units against 3.75 and 4.06 units of experiments using 6.25 and 12.50 wt% GTA, respectively. These results were expectable since plate reader setting were always the same regardless of the sample tested, unlike CLSM experiments where settings were adjusted to the GTA concentrations used to avoid image saturation or signal loss. Alike to what was observed for CLSM, fluorescence levels were independent between samples with varying amounts of BSA for all GTA concentrations used (Table S5). Using 25 wt% GTA concentration, a lower range of $0–50\times10^{-3}$% BSA was tested using this method in discs, retrieving a R^2 = 0.9980 with fluorescence levels remaining independent between different amounts of BSA (Fig. S3 and Table S6). Such high R^2 may be lessened by increasing the number of samples and experiments but confirms the lower detection limit observed by CLSM (6.25×10^{-3}% BSA). Thus, spectrofluorometry data provides the possibility of measuring protein content in both solution and bulk substrates, with acquisition times lower than CLSM. Yet, loss of sensitivity and/or accuracy may occur when using this technique to measure bulk materials.

Conclusions

In this work, a straightforward protocol for quantification of BSA, both in free and immobilized forms, was developed, based on the interaction between BSA and GTA molecules that induces fluorescence emission [2, 18, 21]. This method does not require protein solubilization, in the case of immobilized proteins, nor the use of expensive reagents. Additionally, it is a non-destructive method for the substrate, which is clearly a distinctive feature. Fluorescence profiling of samples containing varying amounts of protein was performed using three different techniques, namely CLSM, spectrofluorometry and widefield fluorescence microscopy. All of them showed a qualitatively and/or quantitatively correlation between fluorescence intensity and the amount of protein after incubation in GTA. Nevertheless, herein, only BSA was tested so future studies should be performed with other proteins known to have GTA-induced florescence. Collectively, this work demonstrates the advantages of an easy, low-cost, in situ method for detection of entrapped and free BSA, without requiring destruction of 3D hydrogel samples. Therefore, in the biomedical field, this method could provide an useful tool to quantify loading/release of BSA in/from hydrogel samples.

Acknowledgements The authors would like to acknowledge FEDER - Fundo Europeu de Desenvolvimento Regional funds through the COMPETE 2020 - Operacional Programme for Competitiveness and Internationalisation (POCI), Portugal 2020, and Portuguese funds through FCT - Fundação para a Ciência e a Tecnologia/ Ministério da Ciência, Tecnologia e Ensino Superior in the framework of the Project PTDC/BBB-BIO/1889/2014, the doctoral grant SFRH/BD/129855/2017 to Mariana I Neves and the contract to Aureliana Sousa in the framework of the project "Institute for Research and innovation in Health Sciences" (POCI-01-0145-FEDER-007274). Marco Araújo gratefully acknowledges Interreg V-A Spain-Portugal (POCTEP) 2014-2020 and FEDER (0245_IBEROS_1_E) for the Postdoctoral grant.

The authors acknowledge the support of Ricardo Vidal from the Biointerfaces and Nanotechnology i3S Scientific Platform, the Bioimaging i3S Scientific Platform, member of the national infrastructure PPBI - Portuguese Platform of Bioimaging (PPBI-POCI-01-0145-FEDER-022122) and Daniela Silva from the Image, Microstructure and Microanalysis Unit (IMCROS) from the Materials Centre of the University of Porto (CEMUP). The authors thank Prof. Nuno Alves from the Centre for Rapid and Sustainable Product Development (CDRSP) of Politécnico de Leiria for the use of the photopolymerization system.

References

1. Sabatini DD, Bensch K, Barrnett RJ (1963) J Cell Biol 17:19
2. Migneault I, Dartiguenave C, Bertrand MJ, Waldron KC (2004) BioTechniques 37:790
3. Shaimi R, Low Siew C (2016) Prolonged protein immobilization of biosensor by chemically cross-linked glutaraldehyde on mixed cellulose membrane. J Polym Eng 36:655
4. Akyilmaz E, Oyman G, Cınar E, Odabas G (2017) Prep Biochem Biotechnol 47:86
5. Sargin İ, Arslan G (2016) Desalin Water Treat 57:10664
6. Zhang M, Zhang Y, Helleur R (2015) Chem Eng J 264:56
7. Aftab K, Akhtar K, Jabbar A (2014) Ecol Eng 73:319
8. Lindén JB, Larsson M, Kaur S, Nosrati A, Nydén M (2016) J Appl Polym Sci 133 n/a
9. Wang W, Jin X, Zhu Y, Zhu C, Yang J, Wang H, Lin T (2016) Carbohydr Polym 140:356
10. Spiller KL, Anfang RR, Spiller KJ, Ng J, Nakazawa KR, Daulton JW, Vunjak-Novakovic G (2014) Biomaterials 35:4477
11. Tamimi E, Ardila DC, Haskett DG, Doetschman T, Slepian MJ, Kellar RS, Vande Geest JP (2015) J Biomech Eng 138:011001
12. Lu W, Ma M, Xu H, Zhang B, Cao X, Guo Y (2015) Mater Lett 140:1
13. Liu Y, An M, Wang L, Qiu H (2014) J Macromol Sci Part B: Phys 53:309
14. Amadori S, Torricelli P, Rubini K, Fini M, Panzavolta S, Bigi A (2015) J Mater Sci Mater Med 26:69
15. Gao S, Yuan Z, Guo W, Chen M, Liu S, Xi T, Guo Q (2017) Mater Sci Eng C 71:891

16. Khalily MA, Goktas M, Guler MO (2015) Org Biomol Chem 13: 1983
17. Habeeb AFSA, Hiramoto R (1968) Arch Biochem Biophys 126:16
18. Bowes JH, Cater CW (1966) J R Microsc Soc 85:193
19. Hopwood D, Allen CR, McCabe M (1970) Histochem J 2:137
20. Hardy PM, Nicholls AC, Rydon HN (1976) J Chem Soc Perkin Trans (1):958
21. Bowes JH, Cater CW (1968) Biochim Biophys Acta 168:341
22. Melo RR, Alnoch RC, Vilela AFL, Souza EM, Krieger N, Ruller R, Sato HH, Mateo C (2017) Molecules 22
23. Rasmussen KE, Albrechtsen J (1974) Histochemistry 38:19
24. Han Y, Duan Q, Li Y, Li Y, Tian J (2018) Adv Polym Technol 37: 1214
25. Gao J, Wu Y, Cui J, Wu X, Meng M, Li C, Yan L, Zhou S, Yang L, Yan Y (2018) J Taiwan Inst Chem Eng 91:468
26. Majorek KA, Porebski PJ, Dayal A, Zimmerman MD, Jablonska K, Stewart AJ, Chruszcz M, Minor W (2012) Mol Immunol 52:174
27. Ma X, Sun X, Hargrove D, Chen J, Song D, Dong Q, Lu X, Fan TH, Fu Y, Lei Y (2016) Sci Rep 6:19370
28. Aston R, Sewell K, Klein T, Lawrie G, Grøndahl L (2016) Eur Polym J 82:1
29. Tahtat D, Mahlous M, Benamer S, Khodja AN, Oussedik-Oumehdi H, Laraba-Djebari F (2013) Int J Biol Macromol 58:160
30. Lu T, Xiang T, Huang X-L, Li C, Zhao W-F, Zhang Q, Zhao C-S (2015) Carbohydr Polym 133:587
31. Chan AW, Whitney RA, Neufeld RJ (2008) Biomacromolecules 9: 2536
32. Yeom CK, Lee K-H (1998) J Appl Polym Sci 67:209
33. Pawar SN, Edgar KJ (2012) Biomaterials 33:3279
34. Bronze-Uhle ES, Costa BC, Ximenes VF, Lisboa-Filho PN (2016) Nanotechnol Sci Appl 10:11
35. Yan J, Wang F, Chen J, Liu T, Zhang T (2016) Int J Police Sci Manag 2016:1
36. Taktak NEM, Awad OM, Elfiki SA, El-Ela NEA (2017) J Macromol Sci Part B: Phys 56:359
37. Kiran Babu SN (2015) J Nanosci Nanotechnol 06
38. Kulkarni AR, Soppimath KS, Aminabhavi TM, Dave AM, Mehta MH (2000) J Control Release 63:97
39. Bio-Rad, "DC™ Protein Assay", http://www.bio-rad.com/en-pt/product/dc-protein-assay. Accessed 20 June 2019
40. T. Scientific, "Pierce™ BCA Protein Assay Kit", https://www.thermofisher.com/order/catalog/product/23225. Accessed 20 June 2019
41. Hou Q, Walsh MC, Freeman R, Barry JJ, Howdle SM, Shakesheff KM (2006) J Pharm Pharmacol 58:895
42. Lima DS, Tenório-Neto ET, Lima-Tenório MK, Guilherme MR, Scariot DB, Nakamura CV, Muniz EC, Rubira AF (2018) J Mol Liq 262:29
43. Wang H, Ying X, Liu J, Li X, Zhang W (2017) J Polym Res:24